

Barium Carboxylate Metal–Organic Framework – Synthesis, X-ray Crystal Structure, Photoluminescence and Catalytic Study

Tanmoy Maity,^[a] Debraj Saha,^[a] Soma Das,^[a] and Subratanath Koner*^[a]

Keywords: Barium / Hydrothermal synthesis / Metal–organic frameworks / Heterogeneous catalysis / Aldol condensation / Photoluminescence

A new 3D alkaline earth metal–organic framework (MOF), [Ba(Hdcp)H₂O]_n (**1**) (H₃dcp = 3,5-pyrazoledicarboxylic acid), has been hydrothermally synthesized and structurally characterized by single-crystal X-ray diffraction analysis. A crystallographic study reveals that each metal ion in **1** is coordinated by eight O atoms and one N atom. Each 3,5-pyrazoledicarboxylate (Hdcp²⁻) ligand coordinates to six alkaline earth metal centers through two carboxylate groups, each of

which adopts a $\mu_3\text{-}\eta_2\text{:}\eta_1$ -bridging coordination mode to afford a 3D network. Thermogravimetric analysis reveals that **1** is thermally stable up to ca. 230 °C. An emission band at ca. 466 nm (λ_{max}) was observed in the photoluminescence spectrum of **1** in the solid state at room temperature. Compound **1** heterogeneously catalyzes the aldol condensation reactions of various aromatic aldehydes with acetone, cyclohexanone, acetophenone, and cyclopentanone.

Introduction

The design and synthesis of functional materials based on metal–organic frameworks (MOFs) have attracted much attention primarily because of their fascinating architectures and potential applications in catalysis,^[1] magnetism,^[2] luminescence,^[3] and gas adsorption and separation.^[4] Dicarboxylate ligands have received increased attention in the construction of coordination-polymer arrays, and the more rigid dicarboxylates in particular are useful building blocks for preparing porous networks with metal ions throughout the periodic system.^[5] The ligand H₃dcp (H₃dcp = 3,5-pyrazoledicarboxylic acid) has six potential donor sites, which involve two nitrogen atoms of the pyrazole ring and four carboxylate oxygen atoms from two carboxylate groups when it is fully deprotonated, and exhibits a multiple coordination motif with the metal center.^[6] A variety of coordination compounds of H₃dcp has been reported, though the majority of them concern transition metals and recently some rare earth cations.^[7] Attempts have been made to study the coordination behavior of main group elements both in aqueous and nonaqueous media, however, only a few of them concern alkaline earth metals.^[6,8] There are two drawbacks in using s-block metals in MOF design: the bonding interaction of s-block metal centers with carboxylate oxygen atoms is mainly ionic in nature due to the large difference in their electronegativities, which provides little

room to predict and control their coordination geometry and their tendency to form solvated metal centers, thus the formation of typical alternating [M(H₂O)₆]L (M = alkaline earth metal, L = ligand) organic–inorganic ionic layers.^[9] In this context, some recent studies concerning the catalytic behavior of alkaline earth metal complexes deserve to be mentioned.^[10] Ana et al. studied alkene hydrogenation and ketone hydrosilylation reactions over alkaline earth sulfonate metal–organic frameworks, which show 100% selectivity towards ethylbenzene under homogeneous conditions.^[10e] They also reported the same reaction over an alkaline earth carboxylate metal–organic framework under heterogeneous conditions.^[10a] Choudary et al. studied an aldol condensation reaction over nanocrystalline magnesium oxide, which showed high activity in the direct asymmetric aldol condensation reaction under heterogeneous conditions.^[11] Baruah et al. studied an aldol condensation reaction catalyzed by magnesium carboxylate compounds under homogeneous conditions.^[10g] Homogeneous catalysts, however, suffer from recyclability problems as the separation of the catalyst from the reaction mixture is troublesome.

In the course of our continuing investigation into the use of MOFs in heterogeneous catalytic reactions, we have successfully employed layered transition metals and lanthanide-based MOFs to catalyze olefin epoxidation reactions.^[12] Recently, we have synthesized a 3D Mg–carboxylate framework, which catalyzes aldol condensation reactions under heterogeneous conditions.^[13] It is of interest to study the catalytic efficacy of barium compounds in aldol condensation reactions. There are several examples of barium-catalyzed C–C bond formation reactions^[14] and some instances of the catalysis of aldol condensation reac-

[a] Department of Chemistry, Jadavpur University, Kolkata 700032, India
Fax: +91-33-2414-6414
E-mail: snkoner@chemistry.jdvu.ac.in
Homepage: www.jaduniv.edu.in/view_department.php?deptid=64
Supporting information for this article is available on the WWW under <http://dx.doi.org/10.1002/ejic.201200417>.

tions.^[14a,14b] However, to the best of our knowledge, there are no reports of barium-containing MOFs that catalyze aldol condensation reactions under heterogeneous conditions. This paper focuses on the preparation and structural characterization of an alkaline-earth-metal-based MOF that affords a new 3D structure involving barium and H₃dcp, namely [Ba(Hdcp)(H₂O)]_n (**1**). Notably, **1** also demonstrates interesting photoluminescence properties.

Results and Discussion

X-ray Structure of [Ba(Hdcp)(H₂O)]_n (**1**)

Single-crystal X-ray diffraction analysis reveals that **1** crystallizes in space group $P2_1/c$ with $Z = 4$. Ba1 is coordinated by nine atoms and has a distorted single capped square-antiprism geometry (Figure 1, a): five oxygen atoms (O1, ⁱO1, O4, ⁱO4, ^eO2) ($g = -x, -y, -z$; $i = x, 1/2 - y, 1/2 + z$) from five different carboxylate anions, two oxygen atoms (O5, ⁱO5) from two bridged water molecules and one oxygen (^eO3) ($e = 1 - x, -1/2 + y, 1/2 - z$) and one nitrogen atom (^cN1) ($c = -x, -1/2 + y, -1/2 - z$) from one five-membered metallocyclic chelate. An ORTEP diagram with atom numbering is shown in Figure S1, and selected bond lengths and angles are collected in Table 1. The Ba–O (carboxylate) bond lengths range from 2.720(3) to 3.047(2) Å, which are consistent with other alkaline earth metal carboxylates.^[10e,15,16] The Hdcp²⁻ ligand has μ_7 connectivity in this structure and each ligand coordinates to six alkaline earth metal centers through two carboxylate groups with a μ_3 - η_2 : η_1 -bridging mode (Figure 1, b), which is similar to that of [Ba(Hpdc)(H₂O)] [Hpdc²⁻ = 3,5-pyrazoledicarboxylate].^[8a] In the previously reported compound [Ba(Hpdc)(H₂O)], two types of barium with different coordination numbers, viz. ten and nine, are connected through an Hpdc²⁻ ligand with μ_7 - and μ_8 -type connectivity. There are three coordinated water molecules and eight coordi-

Table 1. Selected bond lengths [Å] and angles [°] for **1**.

Ba(1)–O(1) 2.848(3)	^e O(3)–Ba(1)–O(4) 87.36(9)
Ba(1)–O(4) 2.722(3)	^e O(2)–Ba(1)–O(4) 126.40(9)
Ba(1)–O(5) 2.900(3)	O(4)–Ba(1)– ^h O(4) 85.05(9)
Ba(1)– ^c N(1) 2.823(3)	ⁱ O(1)–Ba(1)–O(4) 77.20(9)
Ba(1)– ^e O(3) 2.859(3)	O(4)–Ba(1)– ⁱ O(5) 63.60(9)
Ba(1)– ^e O(2) 2.864(3)	O(5)–Ba(1)– ^c N(1) 128.78(10)
Ba(1)– ^h O(4) 2.781(3)	^e O(3)–Ba(1)–O(5) 126.17(9)
Ba(1)– ⁱ O(1) 2.935(3)	^e O(2)–Ba(1)–O(5) 140.01(9)
Ba(1)– ⁱ O(5) 2.817(4)	^h O(4)–Ba(1)–O(5) 61.80(9)
	ⁱ O(1)–Ba(1)–O(5) 68.94(9)
O(1)–Ba(1)–O(4) 132.16(9)	O(5)–Ba(1)– ⁱ O(5) 117.58(9)
O(1)–Ba(1)–O(5) 68.08(9)	^e O(3)–Ba(1)– ^c N(1) 58.73(9)
O(1)–Ba(1)– ^c N(1) 73.41(9)	^e O(2)–Ba(1)– ^c N(1) 67.49(9)
O(1)–Ba(1)– ^e O(3) 126.79(9)	^h O(4)–Ba(1)– ^c N(1) 78.26(9)
O(1)–Ba(1)– ^e O(2) 87.82(9)	ⁱ O(1)–Ba(1)– ^c N(1) 135.89(9)
O(1)–Ba(1)– ^h O(4) 77.74(9)	ⁱ O(5)–Ba(1)– ^c N(1) 113.63(10)
O(1)–Ba(1)– ⁱ O(1) 81.02(9)	^e O(2)–Ba(1)– ^e O(3) 93.79(9)
O(1)–Ba(1)– ⁱ O(5) 141.36(9)	^e O(3)–Ba(1)– ^h O(4) 71.43(9)
O(4)–Ba(1)–O(5) 64.44(9)	ⁱ O(1)–Ba(1)– ^e O(3) 150.64(9)
O(4)–Ba(1)– ^c N(1) 145.44(9)	^e O(3)–Ba(1)–O(5) 82.80(9)
^e O(2)–Ba(1)– ^h O(4) 145.42(9)	^h O(1)–Ba(1)– ^h O(4) 130.59(9)
ⁱ O(1)–Ba(1)– ^e O(2) 76.35(9)	^h O(4)–Ba(1)– ⁱ O(5) 140.29(9)
^e O(2)–Ba(1)– ⁱ O(5) 63.43(10)	ⁱ O(1)–Ba(1)– ⁱ O(5) 68.01(9)

Symmetry transformation codes: (c) $-x, -1/2 + y, -1/2 - z$; (e) $1 - x, -1/2 + y, 1/2 - z$; (g) $-x, -y, -z$; (h) $x, 1/2 - y, -1/2 + z$; (i) $x, 1/2 - y, 1/2 + z$.

nated carboxylate oxygen atoms present in [Ba(Hpdc)(H₂O)]. Amongst them, two water molecules and five carboxylate oxygen atoms are in μ_2 bridging mode. Although one coordinated water and three carboxylate oxygen atoms bridge different types of metals and others bind to the same type of metals. In our case the coordinated water molecule and two carboxylate oxygen atoms (O1 and O4) act as a μ_2 -bridge to connect two metal centers. Here, barium(II) ions are connected by O1, O4, and O5 atoms (and symmetry related ones) to result in a 1D zigzag inorganic chain along the crystallographic c axis (Figure 1, c and d). Bridged oxygen atoms (O1, O4, and O5 and symmetry related ones) share the faces of barium-containing polyhedra

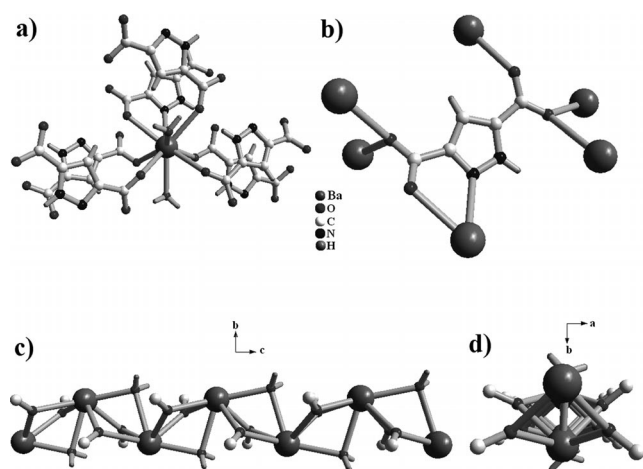


Figure 1. A segment of **1**, showing (a) the local coordination environment of barium(II) ion, (b) the coordination mode of the Hdcp²⁻ ligand in **1**, (c) 1D inorganic chain of **1** along the crystallographic a axis, and (d) along crystallographic c axis.

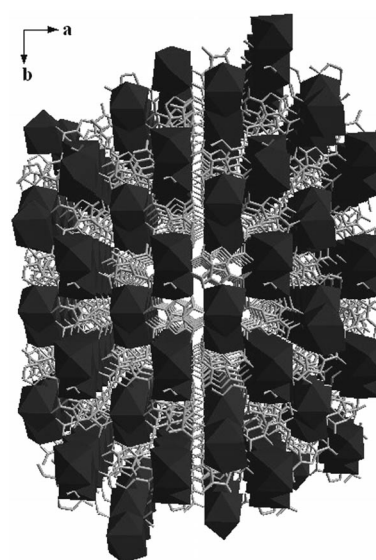


Figure 2. 3D framework of **1**.

with a Ba...Ba distance of 4.24 Å. Organic linkers further connect the 1D chains to create a 3D network (Figure 2). The metal centers are bridged by the organic Hdcp²⁻ linkers to construct a 3D MOF-based binodal 6,6-connected network, considering both the metal centers and Hdcp²⁻ linkers as six-connected nodes (Figure 1, a and b). Additional reinforcement in the networked structure is achieved by two types of intramolecular hydrogen bonds (Table S1) N2–H1...O2 ($-x, 1/2 + y, -1/2 - z$) and O5–H3...O3. Cheetham et al. have introduced a notation rule to categorize the inorganic and organic connectivities in framework structures.^[17] According to this rule the structure can be classified as I¹O² (I = inorganic and O = organic connectivity).

Thermogravimetric Analysis

Thermogravimetric (TG) analysis confirmed that **1** is thermally stable up to ca. 230 °C (Figure 3). The TG curve indicates that **1** starts to lose water molecules at ca. 230 °C. The mass loss of approximately 6% in the temperature range 230–296 °C is in agreement with the theoretical value of 5.8% and corresponds to the loss of one molecule of water. The corresponding differential thermal analysis (DTA) curve shows one endothermic peak at ca. 260 °C. The loss of water at a relatively high temperature indicates that the water molecules are tightly held to the metal centers through a coordination bond. On further heating, the TG curve shows continuous mass loss up to 800 °C due to decomposition of the compound.

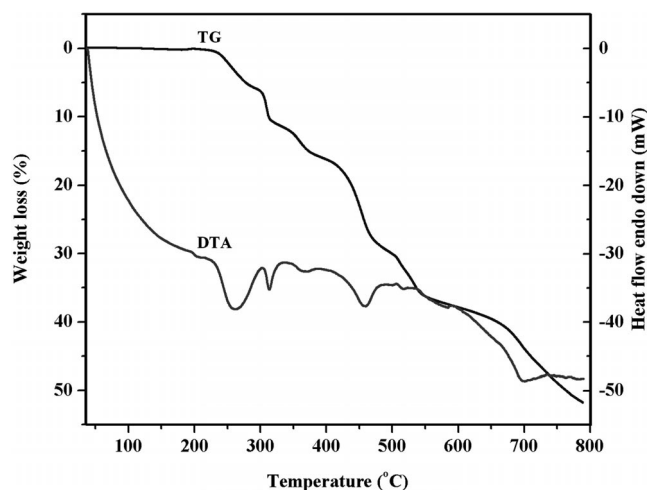


Figure 3. TG-DTA curves of **1**.

Photoluminescence Study

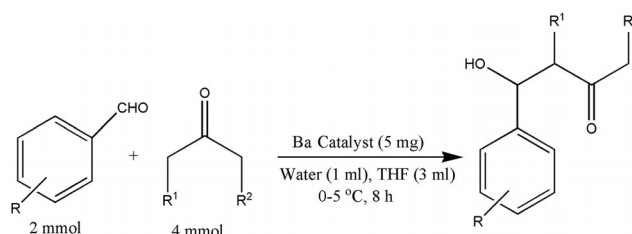
The electronic and photoluminescence spectra of H₃dcp and **1** were measured in the solid state (Figures S2 and S3). The H₃dcp ligand displayed very strong blue fluorescent emission from 370 to 550 nm ($\lambda_{\text{max}} = 425$ nm) upon excitation at 270 nm, which is probably because of a $\pi^* \rightarrow \pi$ electronic transition. In the case of **1**, the emission band was found at 466 nm (λ_{max}) and was redshifted by around

40 nm in comparison to that of H₃dcp. The redshift of the emission spectra observed in **1** in comparison with that of the corresponding free ligand may be attributed to the deprotonation of the ligand in **1**.^[18] This type of photoluminescence can have potential applications in the design of fluorescent materials.^[19] However, examples of barium-based MOFs showing solid state photoluminescence at room temperature are rare.^[8b–8d]

Catalytic Aldol Condensation Reaction

Environmentally friendly, heterogeneous catalytic processes are attracting increasing attention in chemical industries. To find highly active solid Brønsted-type basic catalysts able to perform C–C bond formation remains a challenge. The main drawbacks of using NaOH or KOH as homogeneous catalysts are separation difficulties, corrosion problems in the equipment, and the generation of a large amount of waste. In order to overcome these disadvantages, several efforts have been made to design new catalytic systems with controlled basic properties in order to increase the process efficiency. The catalytic activity of **1** has been studied in aldol condensation reactions under heterogeneous base-free conditions.

Catalytic reactions were performed (Scheme 1) with a large excess of ketone to prevent self-condensation of the aldehyde as well as for effective use of the aldehyde.^[20] Throughout the reaction, the temperature was maintained in the range 0–5 °C. With increasing temperature, benzylideneketone (condensed product) was obtained from the β -aldol. The catalytic reaction was performed in different THF/H₂O ratios (Table S2); the best result was obtained in a 3:1 THF/H₂O mixture, and results of the aldol condensation reactions are summarized in Tables 2 and S3. Under all of the above conditions, aldehydes were converted into their respective β -aldol product, which was the sole product. In this study we noticed that the β -aldol products do not undergo further transformation to form unsaturated carbonyl compounds, which is generally observed.^[21] The yield of the β -aldol product decreased in the order p - > o - > m -nitrobenzaldehyde. It may be realized that the nitro substituent at the *ortho/para* position affords both a negative inductive effect and a negative mesomeric effect, which increases the electrophilicity of the C=O group of these nitrobenzaldehydes, whereas substitution at the *meta* position affords only a negative inductive effect. Between p - and o -



Scheme 1. Reaction scheme of the aldol condensation reaction catalyzed by **1**.

nitrobenzaldehyde, more steric crowding at the *ortho* position may lead to lower conversion for the *ortho* variety. In the case of chloro-substituted benzaldehyde, the β -aldol product obtained from *o*-chlorobenzaldehyde predominates over *m*-chlorobenzaldehyde, which is usual for the effective negative inductive effect in the *ortho* position. Whereas the lower electronegativity of the bromo variety compared to the chloro one causes a lower yield in the case of *m*-bromobenzaldehyde. On the other hand, the presence of an electron-donating group on the ring in the case of the methyl-substituted benzaldehyde, the yield decreases and demonstrates the lowest conversion. Interestingly, in the case of *p*-methoxybenzaldehyde, the yield was still very good. We assume that the methoxy group may interact with

Table 2. Reactions of various aromatic aldehydes and acetone/cyclohexanone catalyzed by **1**.^[a]

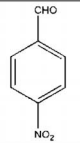
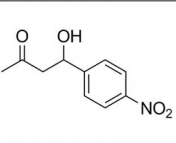
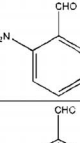
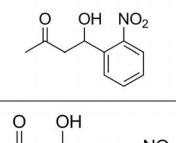
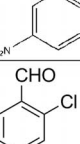
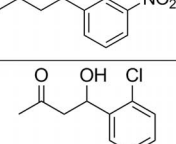
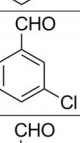
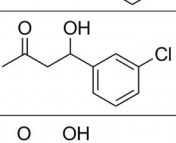
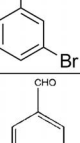
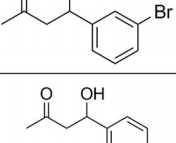
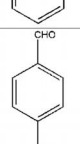
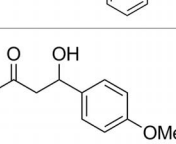
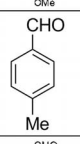
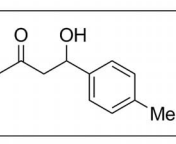
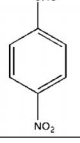
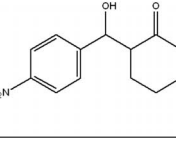
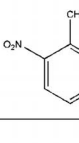
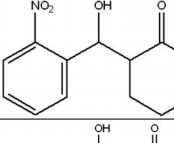
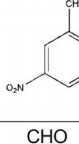
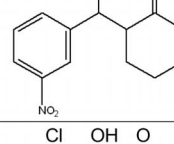
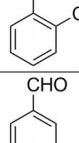
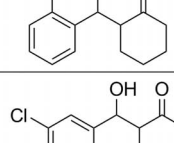
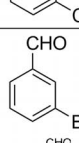
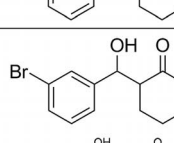
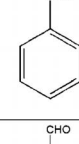
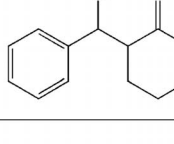
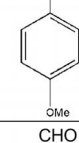
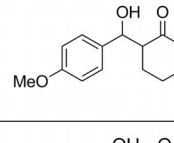
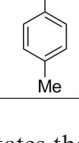
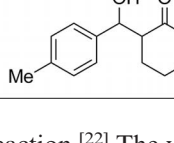
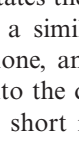
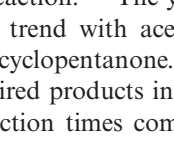
Entry	Ketone	Aldehyde	Major product	Isolated yield (wt.-%)	TON ^[d]
1	acetone			96	120
2	acetone			90	112
3	acetone			80	100
4	acetone			87	109
5	acetone			82	102
6	acetone			74	92
7	acetone			67	84
8	acetone			63	79
9	acetone			52	65
10	cyclohexanone			90	112

Table 2. (Continued)

Entry	Ketone	Aldehyde	Major product	Isolated yield (wt.-%)	TON ^[d]
11	cyclohexanone			85	106
12	cyclohexanone			76	95
13	cyclohexanone			82	102
14	cyclohexanone			77	96
15	cyclohexanone			71	89
16	cyclohexanone			64	80
17	cyclohexanone			59	74
18	cyclohexanone			46	57

barium and facilitates the reaction.^[22] The yields of β -aldol products showed a similar trend with acetone, cyclohexanone, acetophenone, and cyclopentanone. The aldehydes were converted into the desired products in aldol reactions catalyzed by **1** in short reaction times compared to those of other alkaline-earth-metal-catalyzed aldol condensation reactions.^[10g,11] The isolated yields of the products are also higher than those of the magnesium-carboxylate-catalyzed aldol condensation reactions under homogeneous conditions or nanocrystalline-magnesium-oxide-catalyzed asymmetric aldol condensation reactions under heterogeneous conditions. Shibasaki et al. studied similar types of aldol condensation reactions over a barium catalyst under homogeneous conditions, which showed impressive conversion (up to 99%), however the turnover frequencies (TOF) of these reactions are low (0.32–1 h⁻¹).^[24] Besides, the aldol condensation reactions catalyzed by magnesium carboxylate under homogeneous conditions also demonstrate lower TOF values (2–5 h⁻¹) than that of **1**.^[10g]

The BET (Brunauer–Emmett–Teller)^[23] surface area of **1** was calculated from the N₂ adsorption isotherm. The ad-

sorption–desorption isotherm of **1** is shown in Figure S4. The adsorption of N₂ follows a type II isotherm with a surface area (S_{BET}) of 56 m² g⁻¹. This is a consequence of sorption on the surface, not in the framework. Therefore, catalytic reactions clearly take place on the surface of the catalyst rather than in the pores.

Separation, Catalyst Reuse, and Heterogeneity Test

To ascertain that the catalysis was indeed heterogeneous, we performed a hot filtration test. The solid catalyst was filtered when the catalytic reaction was 30–40% complete, and the residual activity of the supernatant solution after separation of the catalyst was studied. The supernatant solution was kept under the reaction conditions for another 8 h, and the composition of the solution was analyzed from time to time. No reaction progress was observed during this period, which excludes the presence of active species in the solution. This experiment clearly demonstrates that there was no leaching of Ba from the solid catalyst during the reactions. Furthermore, atomic absorption spectrometric analysis of the supernatant solution of the reaction mixture collected by filtration confirmed the absence of Ba in the liquid phase.

In order to check the stability of the catalyst, we characterized the recovered material. After the catalytic reactions were completed, the solid catalyst was recovered by centrifugation, washed thoroughly with dichloromethane, and dried under vacuum at 100 °C. The recovered catalyst was then subjected to powder XRD analysis. Comparison of the XRD patterns (Figure 4) of the pristine compound and recovered catalyst convincingly demonstrated that the structural integrity of the compound was unaltered after the reaction.

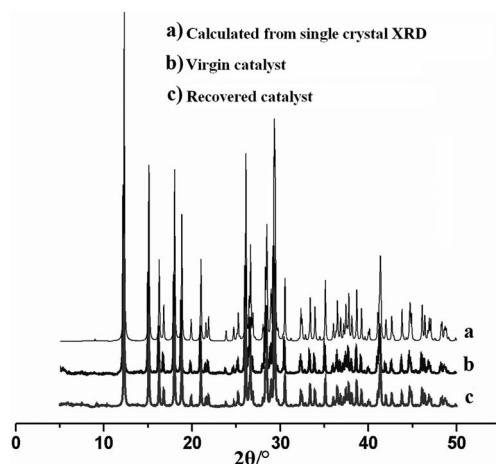


Figure 4. X-ray powder diffraction pattern of virgin and recovered catalyst and calculated diffraction lines for **1**.

For the recyclability study, aldol condensation reactions were performed using *p*-nitrobenzaldehyde with acetone, cyclohexanone, acetophenone, and cyclopentanone. After the first reaction cycle, the catalyst was recovered as mentioned earlier. The performance of the recycled catalyst in up to

five successive aldol reaction runs has been studied (Table S4). The catalytic efficacy of the recovered catalyst remained almost the same in each run.

Conclusions

We have synthesized a new MOF, [Ba(Hdcp)H₂O]_{*n*}, through a hydrothermal route, which is thermally stable up to ca. 230 °C. The compound demonstrates excellent catalytic activity in aldol condensation reactions and displays high yields with 100% selectivity under base free heterogeneous conditions in water/THF. The surface area obtained in the nitrogen sorption measurement indicates that the compound is not porous enough to accept guest molecules in the bulk of the solid. Therefore, the aldol condensation reaction takes place on the surface of the catalyst. However, the advantage of our system is that the catalyst is not air or moisture sensitive; hence, there is no need to carry out reactions under an inert atmosphere. The catalyst can be easily recovered by filtration and can be reused several times without any significant loss of catalytic activity. Future work will continue to focus on constructing alkaline-earth-metal-based frameworks for higher catalytic activity.

Experimental Section

Materials: Barium nitrate, 3,5-pyrazoledicarboxylic acid monohydrate, and substituted benzaldehydes were purchased from Sigma–Aldrich and used without further purification; other chemicals were purchased from Merck (India). Benzaldehyde, acetone, and tetrahydrofuran were distilled before use. Benzaldehyde was kept over NaA molecular sieves to trap possible traces of benzoic acid.

[Ba(Hdcp)H₂O]_{*n*} (1**):** Compound **1** was synthesized through a hydrothermal route. The compound was obtained as colorless block-shaped crystals in a 25 mL teflon-lined Parr acid digestion bomb at 150 °C for 3 d followed by slow cooling to room temperature. The initial reaction mixture was prepared by mixing 3,5-pyrazoledicarboxylic acid monohydrate (0.087 g, 0.5 mmol), lithium hydroxide monohydrate (0.020, 0.5 mmol), and barium nitrate (0.130 g, 0.5 mmol) in milliQ water (8 mL). The crystals obtained were filtered by suction and washed several times with distilled water and then with acetone to remove unreacted materials and dried in air. For characterization of the bulk compound, IR spectroscopy and elemental analysis were undertaken. Selected IR (KBr disk): $\tilde{\nu}$ = 1574 (ν_{as} , CO₂⁻), 1410, 1353 (ν_{s} , CO₂⁻), 1261, 1210, 996, 791 (C–O and O–C–O), 3600 (m, O–H) cm⁻¹. C₅H₄BaN₂O₅ (309.44): calcd. C 19.41, H 1.30, N 9.05; found C 19.4, H 1.4, N 9.0.

X-ray Crystallography: X-ray diffraction data for **1** was collected at 293(2) K with a Bruker SMART APEX CCD X-ray diffractometer using graphite-monochromated Mo- K_{α} radiation (λ = 0.71073 Å). Determination of integrated intensities and cell refinement were performed with the SAINT^[25] software package using a narrow-frame integration algorithm. An empirical absorption correction (SADABS)^[26] was applied. The structure was solved by direct methods and refined using the full-matrix least-squares technique against F^2 with anisotropic displacement parameters for non-hydrogen atoms with the programs SHELXS97 and SHELXL97.^[27] Hydrogen atoms were placed in calculated positions using suitable

FULL PAPER

riding models with isotropic displacement parameters derived from their carrier atoms. In the final difference Fourier maps, there were no remarkable peaks except the ghost peaks surrounding the metal centers. A summary of the crystal data and relevant refinement parameters for **1** is given in Table 3.

Table 3. Crystallographic data and structure refinement parameters for **1**.

Empirical formula	C ₅ H ₄ BaN ₂ O ₅
Formula weight	309.44
Crystal system	monoclinic
Space group	P2 ₁ /c
<i>a</i> [Å]	10.0456(3)
<i>b</i> [Å]	10.5616(3)
<i>c</i> [Å]	7.1981(2)
<i>α</i> [°]	90.00
<i>β</i> [°]	101.3810(10)
<i>γ</i> [°]	90.00
<i>V</i> [Å ³]	748.68(4)
<i>Z</i>	4
Temperature [K]	293(2)
<i>D</i> _{calc} [g cm ⁻³]	2.745
Absorption coefficient [mm ⁻¹]	5.296
<i>F</i> (000)	576
Intervals of reflection indices	-13 ≤ <i>h</i> ≤ 13 -13 ≤ <i>k</i> ≤ 13 -8 ≤ <i>l</i> ≤ 9
Measured reflections	11829
Reflections with [<i>I</i> > 2σ(<i>I</i>)]	1736
Independent reflections	1755
Final <i>R</i> indices [<i>I</i> > 2σ(<i>I</i>)]	<i>R</i> 1 = 0.0310, <i>wR</i> 2 = 0.0805
<i>R</i> indices (all data)	<i>R</i> 1 = 0.0315, <i>wR</i> 2 = 0.0809
<i>R</i> _{int}	0.0160
Δρ _{max} [e Å ⁻³]	0.667
Δρ _{min} [e Å ⁻³]	-3.293
Goodness-of-fit on <i>F</i> ²	1.210

CCDC-872122 contains the supplementary crystallographic data for this paper. These data can be obtained free of charge from The Cambridge Crystallographic Data Centre via www.ccdc.cam.ac.uk/data_request/cif.

Physical Measurement: TG-DTA was performed with a Perkin–Elmer (Singapore) Pyris Diamond TG-DTA unit. Solid state UV/Vis and photoluminescence spectra were recorded with a Shimadzu UV/Vis 1700 spectrophotometer and Fluoro Max-P (Horiba Jobin Yvon) luminescence spectrometer, respectively. The heating rate was programmed at 5 °C min⁻¹ with a protecting stream of N₂ flowing at a rate of 150 mL min⁻¹. Elemental analysis was performed with a Perkin–Elmer 240C elemental analyzer. The FTIR spectrum of a sample in a KBr pellet was measured with a Perkin–Elmer RX I FTIR spectrometer. The metal content of the sample was estimated with a Varian Techtron AA-ABQ atomic absorption spectrometer. Powder XRD patterns of the sample were recorded with a Scintag XDS-2000 diffractometer using Cu-*K*_α radiation. The N₂ gas sorption measurement was performed in the pressure range 0–1 bar with an Autosorb iQ (Quantachrome Inc., USA) gas sorption system. Prior to measurement, the samples were evacuated under dynamic vacuum (10⁻³ Torr) at the desired temperature until a constant weight was achieved. For the isotherm, warm and cold free space correction measurements were performed using ultrahigh purity (UHP) helium gas (99.999% purity). The N₂ isotherm at 77 K was measured in a liquid nitrogen bath using a UHP-grade nitrogen (99.999% purity) gas source.

Catalytic Reactions: The catalytic reactions were carried out in a glass batch reactor according to the following procedure. Ketone

(4 mmol), tetrahydrofuran (3 mL), water (1 mL), and catalyst (5 mg) were combined in a round-bottomed flask. It was then placed in an ice bath and the temperature was maintained at 0–5 °C. To this solution, the requisite amount of aldehyde (2 mmol) was added and the reaction mixture was stirred for 8 h (Scheme 1). After the reaction, the catalyst was separated by filtration, and the filtrate was concentrated in vacuo. The products were purified by column chromatography over silica gel (mesh 60–120) using an *n*-hexane/ethyl acetate mixture as eluent and were analyzed by ¹H NMR spectroscopy, elemental analysis, and by comparing them with authentic samples.

Supporting Information (see footnote on the first page of this article): ORTEP diagram of **1**, results of catalytic reactions in specific condition in tabular form, UV/Vis spectra, N₂ adsorption isotherm, ¹H NMR spectra of all products of known compounds, elemental analysis study of the isolated products.

[a] Reaction conditions: Aldehyde (2 mmol), ketone (4 mmol), tetrahydrofuran (3 mL), water (1 mL), and catalyst (5 mg); *T* = 0–5 °C. Yields were isolated after 8 h of reaction. [d] Turn over number (TON): number of mol converted/mol of active site.

Acknowledgments

We acknowledge the Department of Science and Technology (DST), Government of India for funding a project (to S. K.) (SR/S1/IC-01/2009). T. M. thanks the Council of Scientific and Industrial Research (CSIR), New Delhi, for awarding him a fellowship. Ms. N. Khatun is thanked for her help with NMR spectroscopy. The authors also thank the DST for funding the Department of Chemistry, Jadavpur University to procure a single-crystal X-ray facility and NMR spectrometer under the FIST programme.

- [1] a) S. G. Podkolzin, E. E. Stangland, M. E. Jones, E. Peringer, J. A. Lercher, *J. Am. Chem. Soc.* **2007**, *129*, 2569–2576; b) D. Dang, P. Wu, C. He, Z. Xie, C. Duan, *J. Am. Chem. Soc.* **2010**, *132*, 14321–14323; c) L. Ma, C.-D. Wu, M. M. Wanderley, W. Lin, *Angew. Chem.* **2010**, *122*, 8420; *Angew. Chem. Int. Ed.* **2010**, *49*, 8244–8248.
- [2] a) J. S. Miller, D. Gatteschi, *Chem. Soc. Rev.* **2011**, *40*, 3065–3066; b) Q.-X. Jia, H. Tian, J.-Y. Zhang, E.-Q. Gao, *Chem. Eur. J.* **2011**, *17*, 1040–1051; c) R. Sen, A. Bhattacharya, D. Mal, A. Bhattacharjee, P. Gütllich, A. K. Mukherjee, M. Solzi, C. Pernechele, S. Koner, *Polyhedron* **2010**, *29*, 2762–2768; d) A. Bhattacharjee, Y. Miyazaki, Y. Nakagawa, S. Koner, S. Iijima, M. Sorai, *Phys. B* **2001**, *305*, 56–64.
- [3] a) J. Rocha, L. D. Carlos, F. A. A. Paz, D. Ananias, *Chem. Soc. Rev.* **2011**, *40*, 926–940; b) Y. Cui, Y. Yue, G. Qian, B. Chen, *Chem. Rev.* **2012**, *112*, 1126–1162; c) X.-Z. Song, S.-Y. Song, C. Qin, S.-Q. Su, S.-N. Zhao, M. Zhu, Z.-M. Hao, H.-J. Zhang, *Cryst. Growth Des.* **2012**, *12*, 253–263.
- [4] a) Z. Chang, D.-S. Zhang, Q. Chen, R.-F. Li, T.-L. Hu, X.-H. Bu, *Inorg. Chem.* **2011**, *50*, 7555–7562; b) Y.-W. Li, L.-F. Wang, K.-H. He, Q. Chen, X.-H. Bu, *Dalton Trans.* **2011**, *40*, 10319–10321; c) Z. R. Herm, J. A. Swisher, B. Smit, R. Krishna, J. R. Long, *J. Am. Chem. Soc.* **2011**, *133*, 5664–5667.
- [5] J. L. C. Rowsell, O. M. Yaghi, *Angew. Chem.* **2005**, *117*, 4748; *Angew. Chem. Int. Ed.* **2005**, *44*, 4670–4679.
- [6] J. Xia, B. Zhao, H. S. Wang, W. Shi, Y. Ma, H. B. Song, P. Cheng, D. Z. Liao, S. P. Yan, *Inorg. Chem.* **2007**, *46*, 3450–3458.
- [7] a) L. Pan, N. Ching, X. Huang, J. Li, *Chem. Eur. J.* **2001**, *7*, 4431–4437; b) Y. Wang, Y. Song, Z.-R. Pan, Y.-Z. Shen, Z. Hu, Z.-J. Guo, H.-G. Zheng, *Dalton Trans.* **2008**, 5588–5592; c) A. Zangl, P. Klüfers, D. Schaniel, T. Woike, *Inorg. Chem. Commun.* **2009**, *12*, 1064–1066.

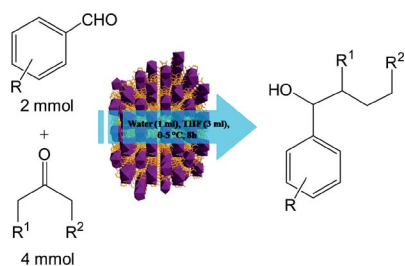
- [8] a) L. Pan, T. Frydel, M. B. Sander, X. Huang, J. Li, *Inorg. Chem.* **2001**, *40*, 1271–1283; b) H.-F. Zhu, Z.-H. Zhang, W.-Y. Sun, T. Okamura, N. Ueyama, *Cryst. Growth Des.* **2005**, *5*, 177–182; c) Y. Yang, G. Jiang, Y.-Z. Li, J. Bai, Y. Pan, X.-Z. You, *Inorg. Chim. Acta* **2006**, *359*, 3257–3263; d) K. M. Fromm, *Coord. Chem. Rev.* **2008**, *252*, 856–885; e) D. Xiao, H. Chen, G. Zhang, D. Sun, J. He, R. Yuana, E. Wang, *CrystEngComm* **2011**, *13*, 433–436.
- [9] a) N. S. Poonia, A. V. Bajaj, *Chem. Rev.* **1979**, *79*, 389–445; b) D. E. Fenton, in: *Comprehensive Coordination Chemistry* (Eds.: G. Wilkinson, R. D. Gillard, J. A. McCleverty), Pergamon, Oxford, **1987**, p. 1.
- [10] a) A. E. Platero-Prats, V. A. de la Peña-O’Shea, M. Iglesias, N. Snejko, Á. Monge, E. Gutiérrez-Puebla, *ChemCatChem* **2010**, *2*, 147–149; b) L. Lin, J. Zhang, X. Ma, X. Fu, R. Wang, *Org. Lett.* **2011**, *13*, 6410–6413; c) L.-H. Wang, *Adv. Mater. Res.* **2011**, *322*, 416–419; d) D. Xiao, H. Chen, G. Zhang, D. Sun, J. He, R. Yuan, E. Wang, *CrystEngComm* **2011**, *13*, 433–436; e) A. E. Platero-Prats, M. Iglesias, N. Snejko, Á. Monge, E. Gutiérrez-Puebla, *Cryst. Growth Des.* **2011**, *11*, 1750–1758; f) C. Brinkmann, A. G. M. Barrett, M. S. Hill, P. A. Procopiou, *J. Am. Chem. Soc.* **2012**, *134*, 2193–2207; g) B. K. Dey, A. Karmakar, J. B. Baruah, *J. Mol. Catal. A* **2009**, *303*, 137–140.
- [11] B. M. Choudary, L. Chakrapani, T. Ramani, K. V. Kumar, M. L. Kantam, *Tetrahedron* **2006**, *62*, 9571–9576.
- [12] a) R. Sen, S. Bhunia, D. Mal, S. Koner, Y. Miyashita, K.-I. Okamoto, *Langmuir* **2009**, *25*, 13667–13672; b) R. Sen, D. K. Hazra, S. Koner, M. Helliwell, M. Mukherjee, A. Bhattacharjee, *Polyhedron* **2010**, *29*, 3183–3191; c) R. Sen, S. Koner, D. K. Hazra, M. Helliwell, M. Mukherjee, *Eur. J. Inorg. Chem.* **2011**, 241–248; d) R. Sen, D. K. Hazra, M. Mukherjee, S. Koner, *Eur. J. Inorg. Chem.* **2011**, 2826–2831.
- [13] R. Sen, D. Saha, S. Koner, *Chem. Eur. J.* **2012**, *18*, 5979–5986.
- [14] a) T. V. Subramanian, B. Jagannadhaswamy, G. S. Laddha, *Indian J. Technol.* **1973**, *11*, 385–387; b) G. Zhang, H. Hattori, K. Tanabe, *Appl. Catal.* **1988**, *36*, 189–197; c) A. Yamaguchi, N. Aoyama, S. Matsunaga, M. Shibasaki, *Org. Lett.* **2007**, *9*, 3387–3390; d) M. Sharma, N. Agarwal, D. S. Rawat, *J. Heterocycl. Chem.* **2008**, *45*, 737–739.
- [15] Y.-C. Gao, Q.-H. Liu, F.-W. Zhang, G. Li, W.-Y. Wang, H.-J. Lu, *Polyhedron* **2011**, *30*, 1–8.
- [16] D. Saha, T. Maity, R. Sen, S. Koner, *Polyhedron* **2012**, *43*, 63–70.
- [17] A. K. Cheetham, C. N. R. Rao, R. K. Feller, *Chem. Commun.* **2006**, 4780–4795.
- [18] P. Yang, J.-J. Wu, H.-Y. Zhou, B.-H. Ye, *Cryst. Growth Des.* **2012**, *12*, 99–108.
- [19] Q. Ye, Y.-H. Li, Y.-M. Song, X.-F. Huang, R.-G. Xiong, Z. Xue, *Inorg. Chem.* **2005**, *44*, 3618–3625.
- [20] J. Lopez, R. Jacquot, F. Figueras, *Stud. Surf. Sci. Catal.* **2000**, *130*, 491–496.
- [21] a) R. K. Zeidan, M. E. Davis, *J. Catal.* **2007**, *247*, 379–382; b) N. Solin, L. Han, S. Che, O. Terasaki, *Catal. Commun.* **2009**, *10*, 1386–1389.
- [22] R. Fernandez-Lopez, J. Kofoed, M. Machuqueiro, T. Darbre, *Eur. J. Org. Chem.* **2005**, 5268–5276.
- [23] S. Brunauer, P. H. Emmett, E. Teller, *J. Am. Chem. Soc.* **1938**, *60*, 309–319.
- [24] Y. M. A. Yamada, M. Shibasaki, *Tetrahedron Lett.* **1998**, *39*, 5561–5564.
- [25] *APEX 2*, *SAINT*, *XPREP*, Bruker AXS Inc., Madison, USA, **2007**.
- [26] *SADABS*, Bruker AXS Inc., Madison, USA, **2001**.
- [27] G. M. Sheldrick, *SHELXS97* and *SHELXL97: Programs for Crystal Structure Solution and Refinement*, University of Göttingen, Germany, **1997**.

Received: April 26, 2012

Published Online: ■

Metal–organic frameworks

The aldol condensation reaction of various aromatic aldehydes is catalyzed by a new 3D alkaline earth metal–organic framework (MOF), [Ba(Hdcp)H₂O]_n (H₃dcp = 3,5-pyrazoledicarboxylic acid). It demonstrates excellent catalytic yields with high selectivity in water/THF under heterogeneous conditions. The catalyst can be recycled and reused several times without significant loss of activity.



T. Maity, D. Saha, S. Das,

S. Koner* 1–8

Barium Carboxylate Metal–Organic Framework – Synthesis, X-ray Crystal Structure, Photoluminescence and Catalytic Study



Keywords: Barium / Hydrothermal synthesis / Metal–organic frameworks / Heterogeneous catalysis / Aldol condensation / Photoluminescence